MIT Open Access Articles

Demonstration of High Performance in Layered Deuterium-Tritium Capsule Implosions in Uranium Hohlraums at the National Ignition Facility

Massachusetts Institute of Technology

Demonstration of High Performance in Layered Deuterium-Tritium Capsule Implosions in Uranium Hohlraums at the National Ignition Facility

T. Döppner,[1] D. A. Callahan,[1] O. A. Hurricane,[1] D. E. Hinkel,[1] T. Ma,[1] H.-S. Park,[1] L. F. Berzak Hopkins,[1]
D. T. Casey,[1] P. Celliers,[1] E. L. Dewald,[1] T. R. Dittrich,[1] S. W. Haan,[1] A. L. Kritcher,[1] A. MacPhee,[1] S. Le Pape,[1]
A. Pak,[1] P. K. Patel,[1] P. T. Springer,[1] J. D. Salmonson,[1] R. Tommasini,[1] L. R. Benedetti,[1] E. Bond,[1] D. K. Bradley,[1]
J. Caggiano,[1] J. Church,[1] S. Dixit,[1] D. Edgell,[2] M. J. Edwards,[1] D. N. Fittinghoff,[1] J. Frenje,[3] M. Gatu Johnson,[3]
G. Grim,[4] R. Hatarik,[1] M. Havre,[5] H. Herrmann,[4] N. Izumi,[1] S. F. Khan,[1] J. L. Kline,[4] J. Knauer,[2] G. A. Kyrala,[4]
O. L. Landen,[1] F. E. Merrill,[4] J. Moody,[1] A. S. Moore,[6] A. Nikroo,[5] J. E. Ralph,[1] B. A. Remington,[1] H. F. Robey,[1]
D. Sayre,[1] M. Schneider,[1] H. Streckert,[5] R. Town,[1] D. Turnbull,[1] P. L. Volegov,[4] A. Wan,[1] K. Widmann,[1]
C. H. Wilde,[4] and C. Yeamans[1]

[1]*Lawrence Livermore National Laboratory, P.O. Box 808, Livermore, California 94551, USA*
[2]*Laboratory for Laser Energetics, University of Rochester, Rochester, New York 14623, USA*
[3]*Massachusetts Institute of Technology Plasma Science and Fusion Center, Cambridge, Massachusetts 02139, USA*
[4]*Los Alamos National Laboratory, P.O. Box 1663, Los Alamos, New Mexico 87545, USA*
[5]*General Atomics, San Diego, California 92121, USA*
[6]*Atomic Weapons Establishment, Aldermaston RG7, United Kingdom*
(Received 17 December 2014; published 28 July 2015)

We report on the first layered deuterium-tritium (DT) capsule implosions indirectly driven by a "high-foot" laser pulse that were fielded in depleted uranium hohlraums at the National Ignition Facility. Recently, high-foot implosions have demonstrated improved resistance to ablation-front Rayleigh-Taylor instability induced mixing of ablator material into the DT hot spot [Hurricane *et al.*, Nature (London) **506,** 343 (2014)]. Uranium hohlraums provide a higher albedo and thus an increased drive equivalent to an additional 25 TW laser power at the peak of the drive compared to standard gold hohlraums leading to higher implosion velocity. Additionally, we observe an improved hot-spot shape closer to round which indicates enhanced drive from the waist. In contrast to findings in the National Ignition Campaign, now all of our highest performing experiments have been done in uranium hohlraums and achieved total yields approaching 10^{16} neutrons where more than 50% of the yield was due to additional heating of alpha particles stopping in the DT fuel.

In indirect-drive inertial confinement fusion (ICF) [1,2], laser energy, converted to thermal x rays inside a high-Z cavity (hohlraum), ablatively drives the implosion of a spherical capsule containing a deuterium-tritium (DT) fuel layer. A high-velocity, low-entropy, highly symmetric implosion is required to form a hot spot of sufficiently high density and temperature from a combination of PdV work and alpha particle deposition. Above the ignition threshold, a self-sustained nuclear burn wave is launched igniting the surrounding compressed fuel layer. Ignition and burn is predicted for stagnation pressures above 300 Gbar [3].

Experiments during the National Ignition Campaign (NIC) [4] demonstrated high implosion velocities ($\sim$360 km/s) [5], and high areal mass densities of 1.3 ± 0.1 g/cm^2 [6], which were predicted to be sufficient to reach ignition [7]. However, some of them showed evidence for significant amounts of CH ablator material mixing into the hot spot [8,9], degrading the implosion performance. To increase the resistance to hydrodynamic instabilities [10], the "high-foot" drive design was developed [11,12], which has demonstrated an order-of-magnitude improvement in

neutron yields with first evidence for additional heating from alpha particle stopping [13]. The high-foot drive raises the hohlraum temperature to 90 eV during the foot, launching a stronger first shock and sets the implosion on a higher adiabat. Among the benefits are a larger ablator density scale length (reducing susceptibility to ablation front Rayleigh-Taylor growth [14]), and a shorter, simplified laser drive (three shocks rather than four). These benefits come at the price of lower fuel areal density, which requires higher implosion velocity compared to the low-entropy design [7] to achieve ignition.

The first high-foot DT implosions [12,13,15] were done in gold (Au) hohlraums. These experiments incrementally increased laser peak power P_{laser} and thus total laser energy from 351 TW/1.3 MJ on N130501 to 428 TW/1.9 MJ on N131119, which is at the current laser energy limit of the National Ignition Facility (NIF). Optimization of the target design is required to further increase the implosion velocity. Another constraint is the shape of the imploded hot spot [16]. With increasing drive it was found that the equatorial shape tends to become more oblate due to reduced inner beam

propagation to the hohlraum waist. To counteract this trend, crossbeam energy transfer (CBET) from the outer to the inner beams can, within a certain limit, be enhanced by increasing the wavelength separation $\Delta\lambda$ between these laser beam groups [17–19]. On the other hand, we want to keep $\Delta\lambda$ low to minimize backscatter and hot electron generation through stimulated Raman scattering (SRS) [20]. Higher-Z (than Au) hohlraums are predicted to help increase the capsule drive at a given P_{laser} and provide a more symmetric hohlraum drive [4]. However, DT experiments using uranium hohlraums during the National Ignition Campaign gave mixed results—they showed one of the best [6] and some of the worst performance, which led us to question the benefits of uranium as a hohlraum material. Herein we will show the benefits of depleted uranium (DU) hohlraums for drive and hot-spot symmetry control compared to standard Au hohlraums in fully integrated DT implosion experiments.

Uranium provides higher opacity and lower specific heat capacity for the hohlraum wall compared to gold [21,22]. Therefore, less laser energy is required to heat the DU hohlraum wall. Any reduction in wall loss increases its reemission (albedo α_w) and thus the hohlraum radiation temperature T_{rad} through the relation

$$P_w = \sigma T_{\text{rad}}^4[(1 - \alpha_w)A_w + A_{\text{LEH}} + (1 - \alpha_{\text{cap}})A_{\text{cap}}]$$
$$- P_{\text{LEH}} - P_{\text{cap}}, \tag{1}$$

with P and A being the powers incident on and areas of the wall, capsule, and LEH (laser entrance hole), respectively, α_{cap} the capsule albedo and σ the Stefan-Boltzmann constant [22]. The first DU hohlraum experiments during the NIC were reported in Refs. [5,19], which quantified the drive enhancement from DU to be equivalent to an additional 6.5% of laser power ($\approx$25 TW) at the peak of the drive compared to Au hohlraums. The impact on hot-spot shape was inconclusive because Au-DU companion implosions were either very prolate [19] or, in the case of high convergence DT implosions, strongly perturbed by jets that originate from the contact ring with the thin plastic tent that is holding the fusion capsule [23].

For the experiments reported here, we use gas-filled hohlraums [Fig. 1(a)] cooled to 18.6 K at shot time [15,24] containing plastic capsules with 2.25 mm outer diameter and 175 μm ("T-1") or 195 μm ("T0") thickness [Fig. 1(d)]. Inside the capsule a smooth, (69 ± 1) μm thick equimolar DT ice layer is grown. The hohlraums are 9.43 mm long and 5.75 mm in diameter and filled with ^{4}He at 1.6 mg/cm^3. They are heated with 192 laser beams, frequency tripled to $\lambda^{(3\omega)} = 351$ nm, through two LEHs of 3.1 mm diameter. The beams are arranged in two cones, the inner cone at 23.5° and 30° and the outer cone at 44.5° and 50° from the vertical hohlraum axis. The wavelengths of the 23.5° beams (λ_{23}), the 30° beams (λ_{30}), and the outer beams (λ_{outer}) can be set independently.

In uranium hohlraums, a nominal 7.0 μm–thick DU layer is encapsulated by gold as shown in Fig. 1(b). The inside surface is lined with 0.7 μm Au, and 22.3 μm Au is added
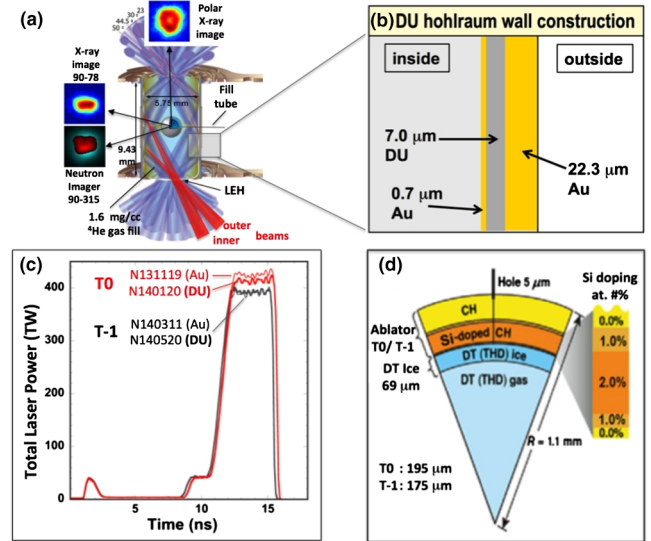

FIG. 1 (color online). Experimental setup for layered DT implosions in DU hohlraums showing the hohlraum wall (b) and the capsule geometries (d). The laser drives (c) are shown for Au-DU comparison experiments with T0 and T-1 CH ablator capsules.

on the outside for structural integrity. The total wall thickness is 30 μm, the same as in Au hohlraums. The thin inside gold layer serves two purposes. First, it acts as a barrier to protect DU from oxidation, which would reduce hohlraum performance. Second, the gold layer is to keep the hohlraum performance the same as in pure Au hohlraums until the main laser pulse arrives. In particular, it allows the use of the same shock timing as in pure Au hohlraums, thus avoiding the need for additional tuning experiments.

Here we focus on the comparison of two layered DU experiments with their companions in Au hohlraums, done with T0 (N131119 vs N140120) and T-1 thickness CH ablator capsules (N140311 vs N140520). Figure 1(c) shows the delivered total laser drive for these experiments; the corresponding companions used the same pulse shape request. The T-1 experiments had a slightly shorter drive due to the reduced shock transit time through the ablator [25]. Au and DU experiments are shown with thin and thick solid lines, respectively. While the delivered laser profile for the T-1 experiments matches very well, it turns out that on N131119 (Au T0) the delivered P_{laser} was 12 TW higher than in the DU experiment N140120 (see Table I). The laser-to-hohlraum coupling η_L is inferred from backscatter measurements [26], where inner beam SRS is the dominant contribution [5]. η_L is slightly reduced on N140120 (DU) vs N131119 (Au) although the difference is within the $\pm$3% error bar [27]. Lower laser delivery and coupling almost compensate the additional drive gain from DU on N140120. As a result, within error bars ($\pm$1.4%), the soft x-ray spectrometer DANTE [28] measured the same peak hohlraum radiation temperature T_R, whereas a T_R increase is seen for the T-1 experiments when going from Au to DU. These trends are corroborated by the times of

TABLE I. Summary of target and drive characteristics along with experimentally measured and inferred (*) performance parameters [29]. Shape metrics are reported from time-integrated hot-spot x-ray emission images.

| | T0 comparison shots | | | T-1 comparison shots | |
	N131119	N140120	N140304	N140311	N140520
Hohlraum	Au	DU	DU	Au	DU
CH capsule thickness (μm)	193.9	195.2	194.1	177.2	178.4
Support tent thickness d_{tent} (nm)	48.1	16.4	45.8	44.5	46.5
Laser peak power P_{laser} (TW)	426	414	442	391	393
Laser energy (MJ)	1.908	1.852	1.863	1.745	1.764
Wavelength separation $\Delta\lambda_{30/23}$ (Å)	8.8/9.5	8.8/9.5	8.8/9.5	6.2/6.9	6.2/6.9
Laser-to-hohlraum coupling η_L	0.871 ± 0.03	0.846 ± 0.03	0.855 ± 0.03	0.857 ± 0.03	0.863 ± 0.03
Peak radiation temperature T_R (eV)	322 ± 4	320 ± 4	327 ± 4	317 ± 4	322 ± 4
X-ray bang time $t_{BT}^{x\,ray}$ (ns)	16.40 ± 0.02	16.37 ± 0.03	16.22 ± 0.02	16.14 ± 0.02	15.91 ± 0.02
X-ray burn width (ps)	152 ± 33	161 ± 28	120 ± 30	115 ± 29	111 ± 25
P_0 (μm) (x ray)	37.5 ± 1.4	32.9 ± 1.3	37.1 ± 1.2	33.8 ± 1.0	27.6 ± 1.4
P_2/P_0 (x ray)	−0.28 ± 0.04	−0.02 ± 0.03	−0.12 ± 0.02	−0.25 ± 0.02	−0.14 ± 0.02
DT Ion temperature T_{ion} (keV) (nToF)	4.83 ± 0.15	5.14 ± 0.15	5.85 ± 0.15	5.36 ± 0.15	5.54 ± 0.15
Downscattered ratio DSR (%)	3.40 ± 0.27	3.71 ± 0.19	3.40 ± 0.22	3.97 ± 0.23	4.08 ± 0.20
DT neutron yield (13–15 MeV) ($\times 10^{15}$)	5.22 ± 0.10	7.98 ± 0.14	8.10 ± 0.15	5.17 ± 0.09	7.63 ± 0.13
Total DT neutron yield* ($\times 10^{15}$)	5.98 ± 0.13	9.25 ± 0.17	9.28 ± 0.19	6.06 ± 0.12	8.98 ± 0.17
Compression yield (kJ)*	9.92 ± 0.50	12.5 ± 0.66	12.3 ± 0.77	9.1 ± 0.44	11.4 ± 0.62
Self-heating yield (kJ)*	6.87 ± 0.64	13.5 ± 0.87	12.8 ± 0.97	7.9 ± 0.57	13.9 ± 0.85
Yield amplification*	1.69 ± 0.10	2.08 ± 0.13	1.96 ± 0.13	1.87 ± 0.10	2.22 ± 0.13
Hot-spot pressure P_{hs} (Gbar)*	123 ± 19	152 ± 25	159 ± 29	140 ± 22	226 ± 37

peak x-ray emission (bang time $t_{BT}^{x\,ray}$). While it is the same within measurement error for the T0 comparison experiments, $t_{BT}^{x\,ray}$ is clearly advanced for the T-1 DU experiment indicating a higher implosion velocity as a result of using DU.

N140120 was the first *high-foot* DT implosion with a DU hohlraum. Despite the effective hohlraum drive being nearly equal to N131119 (Au) its performance greatly improved (see Table I): The primary neutron yield increased by 50% from 5.2 to 8.0×10^{15}, and the ion temperature T_{ion} from 4.8 to 5.1 keV. One of the key observables that clearly improved along with implosion performance was the shape of the hot spot, see Fig. 2 for time-integrated x-ray self-emission (top) and primary neutron emission (bottom). The latter is overlaid with the down-scattered neutron image visualizing the cold DT fuel [30]. The same positive trend for implosion performance and hot-spot shape is observed for the T-1 companion experiments (right panel in Fig. 2). The DU experiments show a 15%–20% higher convergence, and the hot spot is closer to round. As a result, its size from the polar view (M_0) is largely reduced and the doughnut-shaped structure seen on N131119 and N140311 is much less prominent.

A quantitative analysis of the equatorial shape for the dominant P_2 Legendre mode is shown in Fig. 3. The plot includes all no-coasting high-foot DT experiments up to N140520. The ordinate for the T-1 experiments (top axis, open symbols) is shifted by 30 TW to account for the fact that the reduced payload of the thinner capsules requires less drive to accelerate to comparable velocities as in T0 experiments [25]. N130812 and N130927 were done at

smaller $\Delta\lambda$ than the subsequent T0 experiments. Their P_2 values are scaled up as if they were done at the same $\Delta\lambda$ [31,32] to highlight the P_2 trend with P_{laser}. The dashed black line is a linear fit to the Au experiments. It has a slope of $-20\ \mu$m/100 TW; i.e., with increasing P_{laser} the implosions become more oblate. For DU hohlraums the data suggest the same slope. The offset between Au and DU hohlraums is then $\Delta P_2 = (6.5 \pm 1.5)\ \mu$m for a given P_{laser}
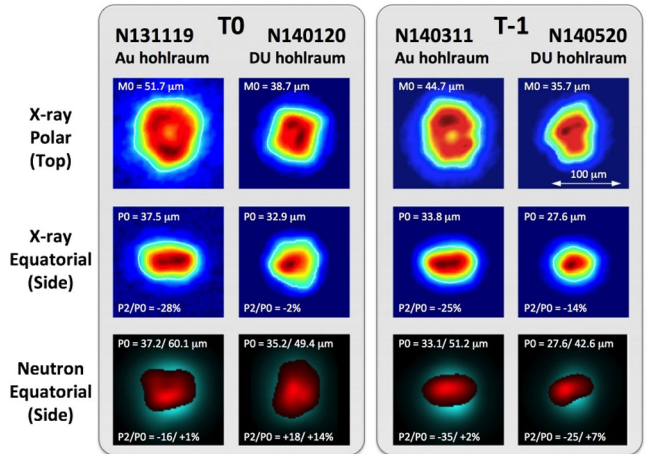

FIG. 2 (color online). Hot-spot shape from time-integrated x-ray (top) and neutron (bottom) images comparing experiments in Au vs DU hohlraums with 195 μm (T0, left panel) and 175 μm thick (T-1, right panel) CH plastic capsules. The lower row shows primary (13–17 MeV, red) and down-scattered (6–12 MeV, turquoise) neutron images overlaid on top of each other with their corresponding shape metrics.
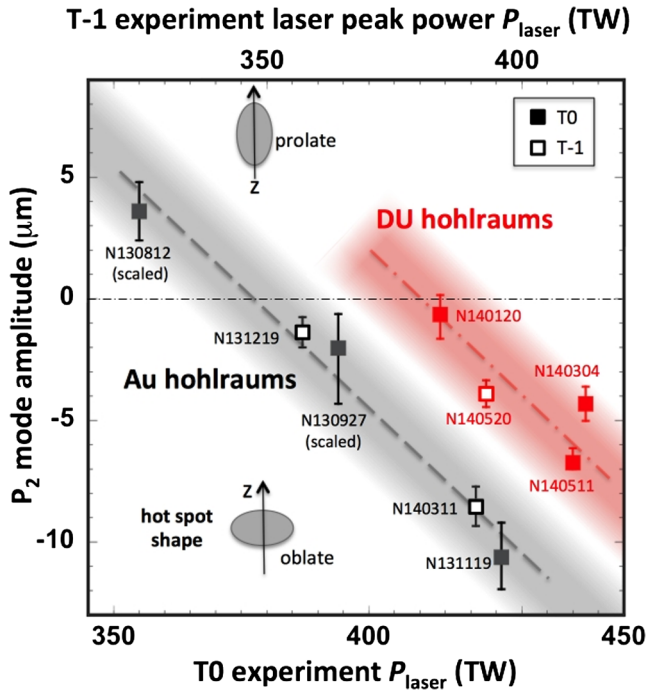
FIG. 3 (color online).   Laser peak power (P_{laser}) scaling of the hot spot P_2 Legendre mode, measured from time-integrated equatorial x-ray emission, for Au and DU hohlraums in layered DT implosions using the high-foot drive with CH ablator capsules of 175 μm (T-1, P_{laser} on top axis) and 195 μm thickness (T0, bottom axis). The DU trend line is 6.5 ± 1.5 μm above the Au trend, i.e., DU allows us to achieve round implosions ($P_2 = 0$) at higher P_{laser}.

and 11.5 μm if the Au-equivalent laser peak powers is conserved, where $P_{laser}^{Au\text{-}eq} = 1.065 \times P_{laser}^{DU}$. While we used the *time-integrated* images for consistency with previous publications, we note that our findings are reproduced when analyzing the *time-resolved* implosion images at peak emission.

All implosions slightly swing towards oblate, typically with $dP_2/dt \sim -2\mu$m/100 ps. This can be explained by a combination of impeded inner beam propagation and reduced CBET starting at ~1.5 ns before the end of the laser drive [15]. N140120 stands out with a 4× larger P_2 swing and, coincidentally, a thinner capsule support tent (16.4 nm vs ~45 nm). It is currently a topic of discussion whether the larger P_2 swing on N140120 is real or possibly a result of a stronger tent perturbation. While lower convergence experiments and simulations show reduced shell perturbations with thinner tents [23,33], simulations also predict larger perturbations for steeper tent departure angles from the capsule surface [34].

The hot-spot shape is a very sensitive diagnostic of any asymmetry in the radiation drive on the capsule. Because these implosions converge more than 30×, they amplify any imperfections in the symmetry of the radiation drive. The symmetry is a complex integrated function of all of the physics of the hohlraum—conversion of laser light into x rays, opacity of the high Z hohlraum wall, heat conduction

to the hohlraum wall, wall motion, laser plasma interactions (e.g., stimulated Raman and Brillouin backscatter, and CBET), and laser beam propagation. Hence experiments, like those reported in this Letter, are crucial to quantify the impact of hohlraum design changes on the implosion shape.

We expect that using DU hohlraums to improve radiation asymmetry and implosion shape because the higher albedo wall reduces the contrast between the portion of the hohlraum wall directly illuminated by laser beams and portions that are not, and in particular reduce the impact of radiation losses through the LEHs. A simple model [4,35] suggests that albedo accounts for +4 μm [see Eq. (44) in Ref. [4]] of the +11.5 μm increase in the P_2 Legendre mode seen in our data. The remaining change in implosion symmetry is likely due to small changes in the other pieces of hohlraum physics.

N140304 was an attempt to further increase the drive for T0 capsules using DU with 28 TW higher P_{laser} compared to N140120. While reduced $t_{BT}^{x\,ray}$ and increased T_{ion} are evidence for higher implosion velocity, the neutron yield did not improve. Reference [31] shows that this is consistent with a model that predicts the yield to scale with absorbed laser energy (rather than P_{laser}). However, it cannot be excluded that other effects like higher preheat from hot electrons or increased residual kinetic energy also contributed.

Figure 4 shows the performance chart of total DT neutron yield vs the downscattered neutron ratio (DSR). Since DSR is directly related to fuel areal density (ρR) [36], Fig. 4 highlights the tradeoff between increased neutron yield at the price of reduced ρR in high-foot implosions compared to low-adiabat experiments during the NIC (gray
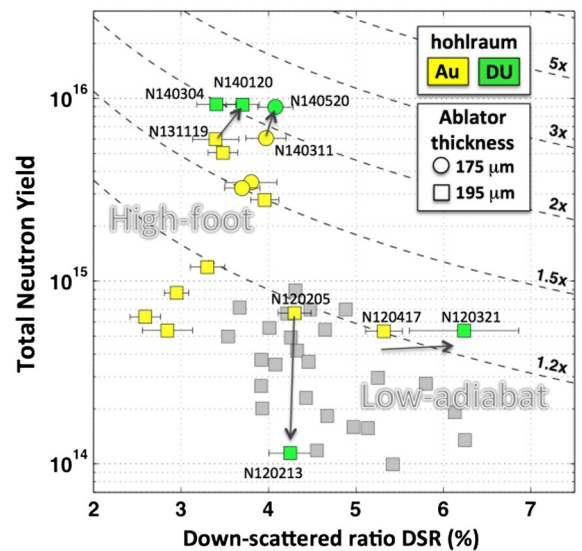

FIG. 4 (color online).   Performance chart of layered DT implosion experiments with CH ablator capsules on the NIF up to N140520 with isocontours for yield amplification due to alpha particle deposition (dashed lines). The highest yield performance was exclusively achieved with uranium hohlraums.

points). About 50% of the latter used DU hohlraums, however, with varying outcome. This is highlighted by two pairs of Au-DU companion experiments. N120205 and N120213 had the same laser pulse request at $P_{\text{laser}} = 440$ TW. While N120205 (Au) performed comparatively well achieving T_{ion} of 3.4 keV, on N120213 (DU) T_{ion} dropped to 1.9 keV and yield plummeted by a factor of 6× due to CH ablator material catastrophically mixing into the hot spot [8]. Conversely, the highest DSR and thus fuel ρR reported so far was achieved with a DU hohlraum on N120321 [6]. It had the same Au-equivalent hohlraum drive at $P_{\text{laser}}^{\text{Au-eq}} = 370$ TW as N120417 (Au), resulting in the same neutron yield on these companion experiments. The higher DSR on N120321 can be explained by details in the delivered laser drive resulting in slightly different shock timing [37].

Thanks to the strongly reduced instability growth in the high-foot drive design [14] the twofold advantage of DU hohlraums becomes visible. Not only that they help to increase drive and implosion velocity, but they also allow us to achieve round implosions ($P_2 = 0$) at higher peak laser power. All three DU experiments discussed in this Letter each generated a total of 9×10^{15} neutrons, ca. 50% more than any experiment in a gold hohlraum. From experimental hot-spot observables we infer [13] that, for the first time, more than 50% of the neutron yield is due to additional heating from alpha particles depositing their energy into the hot spot. While it has to be cautioned that this inference is based on 1D hot-spot models, power scaling of yield with implosion velocity and hot-spot pressure is further evidence for this amount of alpha particle contribution [31,38].

These first DU experiments were a turning point in the high-foot campaign. Despite significantly higher target fabrication requirements, all subsequent layered implosion experiments aiming at highest performance have used DU hohlraums. In the future, new hohlraum shapes are explored that will allow better control of the implosion shape at reduced CBET and hot electron generation like Rugby-shaped hohlraums [39]. Additionally, modifications of the high-foot drive design are proposed, which lower the laser drive after the picket in order to keep the fuel at a lower adiabat allowing for higher final fuel compression [40].

[1] J. D. Lindl, P. Amendt, R. L. Berger, S. G. Glendinning, S. H. Glenzer, S. W. Haan, R. L. Kauffman, O. L. Landen, and L. J. Suter, Phys. Plasmas **11**, 339 (2004).
[2] S. Atzeni and J. Meyer-Ter-Vehn, *The Physics of Inertial Fusion* (Oxford University Press, Oxford, 2004).
[3] B. K. Spears et al., Phys. Plasmas **19**, 056316 (2012).
[4] J. Lindl, O. Landen, J. Edwards, E. Moses, and NIC team, Phys. Plasmas **21**, 020501 (2014).
[5] J. L. Kline et al., Phys. Plasmas **20**, 056314 (2013).
[6] V. A. Smalyuk et al., Phys. Rev. Lett. **111**, 215001 (2013).
[7] S. W. Haan et al., Phys. Plasmas **18**, 051001 (2011).
[8] T. Ma et al., Phys. Rev. Lett. **111**, 085004 (2013).
[9] S. P. Regan et al., Phys. Rev. Lett. **111**, 045001 (2013).
[10] T. C. Sangster et al., Phys. Plasmas **20**, 056317 (2013).
[11] T. R. Dittrich et al., Phys. Rev. Lett. **112**, 055002 (2014).
[12] H. S. Park et al., Phys. Rev. Lett. **112**, 055001 (2014).
[13] O. A. Hurricane et al., Nature (London) **506**, 343 (2014).
[14] D. T. Casey et al., Phys. Rev. E **90**, 011102 (2014).
[15] O. A. Hurricane et al., Phys. Plasmas **21**, 056314 (2014).
[16] G. A. Kyrala et al., Phys. Plasmas **18**, 056307 (2011).
[17] P. Michel et al., Phys. Rev. Lett. **102**, 025004 (2009).
[18] S. H. Glenzer et al., Science **327**, 1228 (2010).
[19] D. A. Callahan et al., Phys. Plasmas **19**, 056305 (2012).
[20] P. Michel et al., Phys. Rev. E **83**, 046409 (2011).
[21] J. Schein, O. Jones, M. Rosen, E. Dewald, S. Glenzer, J. Gunther, B. Hammel, O. Landen, L. Suter, and R. Wallace, Phys. Rev. Lett. **98**, 175003 (2007).
[22] O. S. Jones et al., Phys. Plasmas **14**, 056311 (2007).
[23] R. Tommasini et al., Phys. Plasmas **22**, 056315 (2015).
[24] S. H. Glenzer et al., Phys. Plasmas **19**, 056318 (2012).
[25] T. Ma et al., Phys. Rev. Lett. **114**, 145004 (2015).
[26] J. D. Moody et al., Rev. Sci. Instrum. **81**, 10D921 (2010).
[27] Backscatter diagnostic participation is reduced on high neutron yield shots, and for inner SRS relies on the full aperture backscatter measurement on one inner 30° quad. This leads to a larger uncertainty in total backscatter and thus in coupling η_L (±3%) than reported in Refs. [5,26] (±2%). The ±3% error corresponds to the 1σ confidence interval, which is estimated from shot-to-shot fluctuations in backscatter in a sample of 15 identical hohlraum experiments (same hohlraum and laser drive request).
[28] N. B. Meezan et al., Phys. Plasmas **20**, 056311 (2013).
[29] Because of an unfold correction for the neutron time-of-flight signals on high-yield experiments the values for T_{ion} and DSR for N131119 were updated compared to Refs. [13,15].
[30] F. E. Merrill et al., Rev. Sci. Instrum. **83**, 10D317 (2012).
[31] D. A. Callahan et al., Phys. Plasmas **22**, 056314 (2015).
[32] N130812 (355 TW, $\Delta\lambda_{30/23} = 7.3/8.5$ Å) and N130927 (397.5 TW, $\Delta\lambda_{30/23} = 8.5/9.2$ Å) were done at smaller $\Delta\lambda = (\Delta\lambda_{30} + \Delta\lambda_{23})/2$ than the four high-power shots (N131119/N140120/N140304/N140511: $\Delta\lambda_{30/23} = 8.8/9.5$ Å), where $\Delta\lambda_{30}$ ($\Delta\lambda_{23}$) is the difference in fundamental wavelength between the outer beams and the 30° (23°) beams. We rescaled P_2 for N130812 (+10.6 μm) and N130927 (+3.2 μm) to $\Delta\lambda = 9.15$ Å by using the experimentally observed trend, which is (8.5 ± 1.0) μm towards prolate shape per 1 Å increase in $\Delta\lambda$ [31].
[33] S. R. Nagel et al., Phys. Plasmas **22**, 022704 (2015).
[34] B. A. Hammel et al., Bull. Am. Phys. Soc. **59** (2014); http://meeting.aps.org/Meeting/DPP14/Session/UO4.7.
[35] O. L. Landen et al., Phys. Plasmas **6**, 2137 (1999).
[36] J. A. Frenje et al., Nucl. Fusion **53**, 043014 (2013).
[37] H. F. Robey et al., Phys. Plasmas **20**, 052707 (2013).
[38] O. Hurricane et al. (to be published).
[39] P. Amendt et al., Phys. Plasmas **21**, 112703 (2014).
[40] J. L. Peterson, L. F. Berzak Hopkins, O. S. Jones, and D. S. Clark, Phys. Rev. E **91**, 031101 (2015).